Applications of inverse gas chromatography in the study of liquid crystalline stationary phases

Gareth J. Price*, Simon J. Hickling, Ian M. Shillcock

Department of Chemistry, University of Bath, Claverton Down, Bath BA2 7AY, UK

Abstract

We describe measurements on a number of low-molar-mass and polymeric liquid crystals that contain the same mesogenic groups. Transition temperatures for the mesophases have been measured and the supercooled region of hexyloxycyanobiphenyl studied, revealing some differences from the stable mesophase. Activity coefficients and interaction parameters for a range of probes have been measured and allow us to determine the nature and origin of the thermodynamic interactions in the systems. A discussion of how this fundamental information can be used in designing more efficient stationary phases for analytical gas chromatography is also presented.
© 2002 Elsevier Science B.V. All rights reserved.

1. Introduction

Liquid crystalline compounds (LCs) have been developed into a very useful class of materials [1,2]. Both small molecules with mesogenic properties and polymers, which may show LC behaviour due to the main chain configuration or be substituted with mesogenic groups, are used. Liquid crystalline phases occur where, above the melting point, some molecular order is retained in the fluid. In general, they are formed from compounds that have elongated, rod-like molecules. Thermotropic LCs display this behaviour as a function of temperature and some of the molecular arrangements that can be adopted are shown in Fig. 1. For many applications, polymeric LCs are preferred for their better thermal stability and/or ease of processing. However, suitable systems are not always available and for some

applications polymer-dispersed LCs are used where small molecules LCs are surrounded by a glassy polymer. Other applications demand LCs dissolved in a polymer or carrier; these include dyes, coatings and films. Some years ago, LCs and LC polymers (LCPs) were suggested as stationary phases for analytical gas chromatography where the molecular ordering of the LCs should allow discrimination between closely related isomeric analytes. For each of these applications, knowledge of the interactions between the components is important in designing and formulating new systems.

We are involved in a programme investigating a range of LCs as potential stationary phases. This paper presents some of our work aimed at quantifying interactions in LC containing materials. The ability to characterise retention in each of the various mesophases is important so this will feature in the initial discussion. In order to optimise stationary phase behaviour, the nature and origin of the interactions between the analytes and the LCs will need to

*Corresponding author. Fax: +44-1225-826-231.
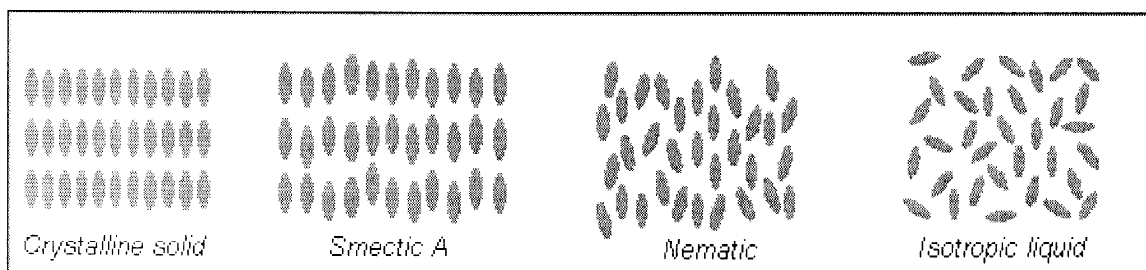*E-mail address:* g.j.price@bath.ac.uk (G.J. Price).

Fig. 1. Liquid crystalline phases displayed with increasing temperature.

be understood and this will be illustrated in the next section of the paper. Finally, given the recent trends toward GC operation at high analysis temperatures, the use of polymeric materials is preferred, so we will briefly investigate the relationship between retention in polymeric LC systems with their low-molar-mass equivalents. This paper will describe some of our work in this area to give the reader an overview of the types of measurements that are possible and necessary for the development of LC phases.

2. Theory and background

Inverse gas chromatography (IGC) has been used to investigate the physicochemical properties of a wide range of systems including polymers [3,4]. The fundamental datum obtained by IGC is the specific retention volume, V_g^0, the volume of carrier gas under standard conditions required to elute the probe per gram of stationary phase [5]. It was shown some years ago by Everett [6] that, at infinite dilution, V_g^0 could be related to the thermodynamics of the probe–stationary phase interaction:

$$\ln \gamma^\infty = \ln \frac{273.15R}{V_g^0 p_1^0 M_2} - \frac{p_1^0(B_{11} - V_1)}{RT} \qquad (1)$$

where γ^∞ is the molar activity coefficient of the probe at infinite dilution, p^0 is the saturated vapour pressure of probe at temperature T, B_{11} is the second virial coefficient of the probe vapour, V_1^0 is the molar volume of the probe and M_2 the molar mass of the stationary phase. It is also readily shown that V_g^0 is

related to the Gibbs energy of solution of the probe in the stationary phase by:

$$\Delta G^{sol} = -RT \ln V_g^0 - C = \Delta H^{sol} - T\Delta S^{sol} \qquad (2)$$

where C is a constant dependent on the choice of reference state. From Eqs. (1) and (2), a number of other thermodynamic parameters such as enthalpies and entropies of solution and mixing readily follow using standard relationships [5].

However, calculation of the activity coefficients presents problems when considering a polymer. Eq. (1) requires an accurate molar mass for the determination of the molar activity coefficient. Often this is not known for polymer solutions and all synthetic polymers pose the added problem of polydispersity. Also, early work on long chain alkane stationary phases [7] gave activity coefficients which became increasingly dependent on molecular mass as the chain length increased, which was at variance with the asymptotic behaviour of the observed physical parameters. Patterson et al. [7] circumvented this problem by introducing a weight fraction based activity coefficient, Ω, which better describes the observed behaviour of the solutions:

$$a = \gamma x = \Omega w \qquad (3)$$

where x and w are the mole and weight fractions of a component, respectively. The weight activity coefficient has become the most widely used parameter in IGC of polymers and can be calculated from chromatographic data using the molar mass of the probe, M_1 and:

$$\ln \Omega^\infty = \ln \frac{273.15R}{V_g^0 p_1^0 M_1} - \frac{p^0(B_{11} - V_1)}{RT} \qquad (4)$$

When considering polymers, it is convenient to use the Flory–Huggins interaction parameter, χ. This represents the free energy of mixing due to other than simple mixing considerations. It may be calculated from:

$$\chi^{\infty} = \ln \Omega^{\infty} - \left(1 + \frac{V_1^0}{V_2^0}\right) + \ln\left(\frac{M_1 V_2^0}{M_2 V_1^0}\right) \qquad (5)$$

The possibility of using the ordered LC structures for analytical purposes was realised some years ago. It was suggested that, to exhibit good separation and column efficiency, nematic phases were best, although a number of other phases have been used [8]. Kelker [9] first recognised that mesophases were good stationary phases for geometric isomer separation and managed to resolve all three xylene isomers. Since then, mesophases have been widely applied to a large range of separations [10–14]. Applications to which liquid crystal stationary phases have been applied include separations of isomers of benzene, alkanes, alkenes, heterocycles, poly-aromatic hydrocarbons, polychlorinated biphenyls, and benoxaprofen isomers, as reviewed by Witkiewicz and Mazur [14]. In parallel with the growth of polysiloxane stationary phases for a wide range of analyses, liquid crystalline versions—MEPSILs—have been developed and a number of these materials have been studied [15,16].

The thermodynamics of interactions in LC systems are more complex than in isotropic solutes. Chow and Martire [17] developed a model for the activity coefficient of a probe in a mesophase system, based upon internal energy changes upon forming a solution, and this has since been developed in a more general theory and has been applied to analytical systems [18–20].

One of the most commonly studied LC systems is the alkyl- or alkoxy-substituted cyanobiphenyls which have been widely used in display applications. Martire and co-workers [21,22] have studied a series of alkylcyanobiphenyl molecules, characterising them in terms of activity coefficients and the associated enthalpies and entropies associated with the solution process. A comparison of the behaviour of siloxane-substituted cyanobiphenyls with low-molar-mass equivalents has been reported briefly by Price and Shillcock [23] and the work in this paper extends

that study. A very recent study [24] has attempted to correlate IGC measured diffusion coefficients with mesophase structure in some nematic LCs.

There have been few studies of LC polymers, particularly where the mesogen is attached to the polymer in a side chain [15,23]. Main chain LCPs, which have the mesogenic group as part of the backbone of the polymer, have also been studied by IGC [25–27]. However, in the main these materials have not been used for analytical applications and have not been further considered in the work described in this paper.

3. Experimental

A modified Pye Unicam 204 chromatograph fitted with flame ionization detection (FID) and modified to allow the column inlet and outlet pressures to be measured was used for the chromatographic measurements. The usual checks were made to confirm that work was performed in the infinite dilution region [4]. Nitrogen, with flow-rates between 15 and 80 cm^3 min^{-1} was used as the carrier gas into which ~0.01–0.05-μl samples of the probe vapours were injected from a syringe. The probes were of analytical grade and were obtained from Aldrich (Poole, UK). The mean of at least three measurements of their retention times agreeing to within experimental uncertainty was recorded to ±0.01 min with a Spectra-Physics SP4270 integrator. No dependence on the amount of probe injected was noted for any system reported here. The column temperature was monitored to ±0.1 °C using a thermocouple that had been calibrated against a Tinsley Type 5840 platinum resistance thermometer. The temperature variation through the oven was less than 0.2 °C.

The structures of the compounds used as stationary phases are shown in Fig. 2. The acronyms which will be used to identify each of the LCs used are also shown. The nematic, N, phases of 4-n-octyloxy(4′-cyanobiphenyl) (OCB) and 4-n-hexyloxy(4′-cyanobiphenyl) (HCB) possess orientational order along the direction of the long axis of the molecule. Poly-(dimethyl - co - methyl(4 - cyanobiphenyloxy)butyl-siloxane) (PDCBBS) and OCB exhibit a smectic A, S_A, phase where in addition to the alignment, the
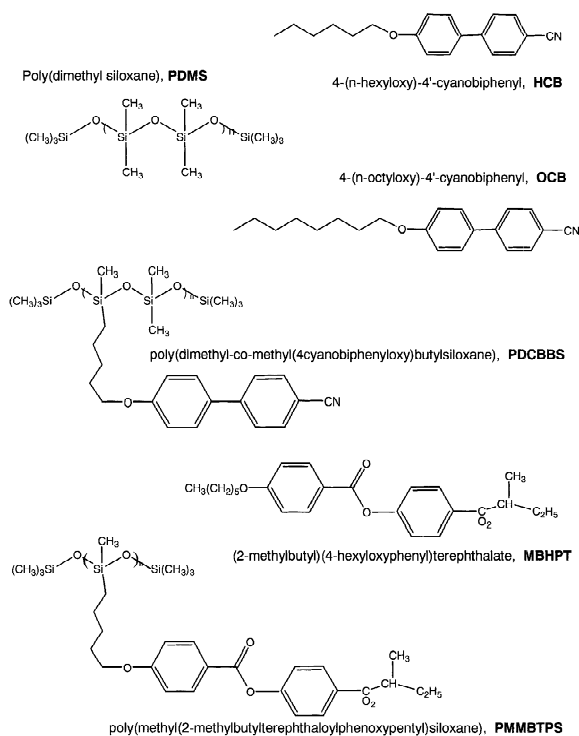
Fig. 2. Structures and acronyms of liquid crystalline phases used.

mesogens are oriented in layers. The LCs were supplied by Merck (Poole, UK).

The stationary phases were prepared in the usual way by coating the support from chloroform solution onto Chromosorb P of 100–120 mesh size. The resulting phase was dried to constant weight and a known amount packed into 0.25-inch O.D. copper tubing (1 inch=2.54 cm). The exact amount of liquid crystal on the column was determined by calcination or, for the siloxane polymers, by exhaustive soxhlet extraction. Loadings in the range of 8–16% (w/w) were used. Within this range, no significant variation of retention with loading was observed.

4. Results and discussion

Experimentally measured retention times, t_R, were converted [5] to specific retention volumes, V_g^0, using:

$$V_g^0 = \frac{(t_R - t_M)F'J}{W} \qquad (6)$$

where t_M is the retention time of a non-interacting marker, F' is the carrier flow-rate corrected to STP, J is the correction for gas compressibility and W the mass of stationary phase on the column. F' was calculated from the measured flow-rate, F, obtained at laboratory conditions and corrected for the laboratory temperature, T, and atmospheric pressure, p^0 as well as for water vapour pressure, $p^{w,}$ in the flowmeter using literature constants [28].

$$F' = F \cdot \left(\frac{273.15}{T}\right) \cdot \left(\frac{760}{p^0}\right) \cdot \left[1 - \left(\frac{p^w}{p^0}\right)\right] \qquad (7)$$

The correction factor for gas compressibility is given in terms of the column inlet and outlet pressures, p^i and p^o respectively, by [29]:

$$J = \frac{3}{2} \cdot \left[\frac{\left(\frac{p^i}{p^0}\right)^2 - 1}{\left(\frac{p^i}{p^0}\right)^3 - 1}\right] \qquad (8)$$

4.1. Phase transition behaviour

One of the most common methods for determining the phase transition is differential scanning calorimetry (DSC). The DSC measurements of the transition temperatures for HCB, OCB and PDCBBS have been described previously [30]. Those for (2-methylbutyl)(4-hexyloxyphenyl)terephthalate (MB-HPT) and poly(methyl(2-methylbutylterephthaloyl-phenoxypentyl)siloxane) (PMMBTPS) showed similar properties. In order to confirm the applicability of measurements on the LCs when coated onto the Cromosorb support, both the bulk materials and samples of the IGC stationary phases were investigated. The coated materials showed transition temperatures on average 1 °C lower than those measured for the bulk materials. While this is within the experimental uncertainty of the measurements, it may indicate that the support exerts some influence on the LC phase behaviour. However, any effect, if one is present, is clearly very small.

The phase behaviour of the LCs was investigated by measuring the IGC retention of a range of hydrocarbon probes with differing shape and polar-

isability. More polar probes, such as chloroform, are very good solvents for the materials used here. In their studies on polymer transitions, Llorente et al. [31] reported that such probes interfere with transitions by dissolving in the lower temperature phase. This would not have been the case for the non-polar hydrocarbons so that the results should be more meaningful. An example of the Van't Hoff plots obtained is shown for OCB in Fig. 3. This compound shows each of the mesophase types displayed by the LCs involved in this work.

As expected, the retention volume generally decreases as the temperature increases. About the melting point of the solid, retention increased considerably as the probe was able to absorb into the bulk material rather than surface adsorption being the only available retention mechanism. Retention then decreased again with further, smaller, increases in retention about subsequent phase transitions until the isotropic phase was reached, whereupon retention continued to fall with increasing temperature. This behaviour has been observed in a number of liquid crystal systems [32–34]. For OCB the smectic A to nematic phase transition was accompanied by a small but significant increase in retention volume. This is a consequence of the relatively small change in the molecular order of the LC between the two phases affecting the interactions, as discussed below.

The crystalline to mesophase transitions exhibited a small degree of pre-melting behaviour, manifested as an increase in retention volume prior to the transition temperature. No hysteresis was observed,
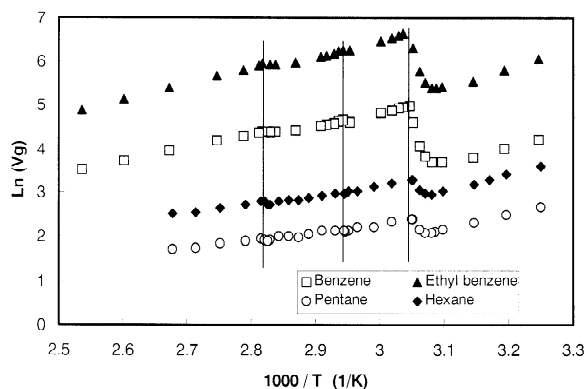
within experimental uncertainty, for the higher temperature mesophase transitions but considerable hysteresis occurs about the crystalline transition and, as the LC mesophase is cooled it enters a supercooled phase. Further discussion of these factors will be included in the next section of this paper.

Fig. 4 shows the retention diagram for PMMBTPS. The glass transition temperature was measured by DSC to be −7 °C; however, the present IGC apparatus is not capable of sub-ambient operation so that this value is not observed. The mesophase transition is though clearly apparent. The temperature range over which the transition occurs is larger for the polymer due to the polydispersity of the material. However, the transition is more pronounced in the polymeric material, suggesting the siloxane backbone plays a role in solvation. In this case, no significant difference was detected for the two probes.

In some cases, the transitions were rather difficult to detect from the Van't Hoff plots. This is not surprising since the basis of the method is related to that used for measuring glass and melting transitions in polymers. These involve large changes in the structure of the materials involved whereas here very small, subtle changes in molecular orientation are occurring during mesophase transitions. Differences in retention between the mesophases are due to differing thermodynamic interactions with the probe as will be discussed below. Thus, consideration of the thermodynamic properties is more likely to differentiate between the phases. An example is shown in Fig. 5 which shows the activity coefficient plots for hexane and benzene as examples of the

Fig. 3. Van't Hoff retention diagram for four probes in OCB. The vertical lines indicate the phase transition temperatures.
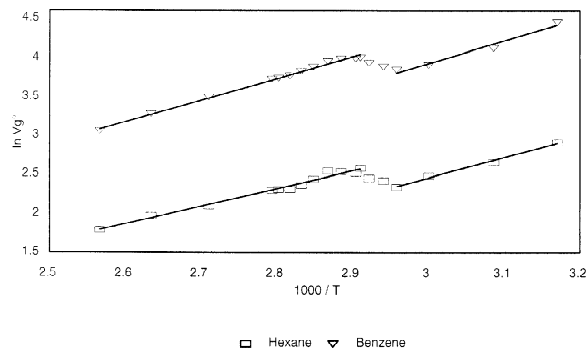

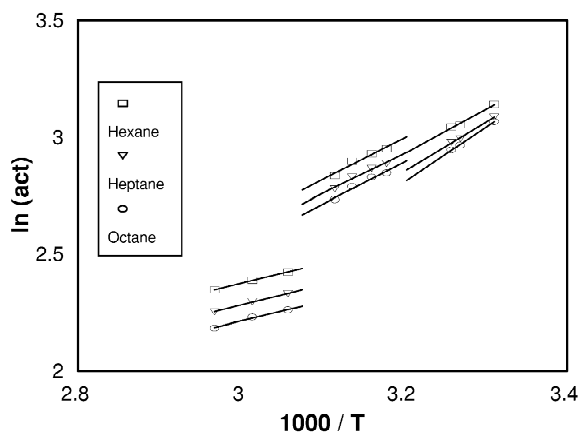Fig. 4. Van't Hoff retention diagram for probes in PMMBTPS.

Fig. 5. Activity coefficient–reciprocal temperature plot for MBHPT.

probes used. Note that this data was measured with reducing temperatures and so the large melting transition is not seen. Again, there is a distinct change in the gradient observed on the retention diagram. The transition temperatures as obtained from the plot of $\ln \Omega^\infty$ vs. $1/T$ were identical to those estimated from the plot of $\ln V_g^0$ vs. $1/T$ within relatively large experimental uncertainty of the latter.

It is important in this type of work to ensure that the results are not probe dependent. The transition temperatures were taken as the temperature at which the lower temperature phase no longer exists, corresponding to the retention maximum about the transition. The transition temperatures for the various probes in the OCB and PDCBBS are listed in Tables 1 and 2. For these LCs, no significant difference was found for the probes used. The reproducibility and precision are comparable with those found from hot stage microscopy (HSM), DSC, or density measurements.

A comparison of the transition temperatures obtained by DSC and IGC is shown in Table 3. In general, there is very good agreement between the various methods. The only significant difference occurs with MBHPT. The results obtained by DSC shows the K→S_C transition to occur at a slightly depressed temperature, compared with the results obtained from IGC. The excellent agreement of the other results for this compound suggest that this is not due to a support effect but may be due to the aromatic probe having a greater affinity for the LC

Table 1
Transition temperatures[a] (°C) for OCB measured for different probes

	T_{NI}	T_{NS}	T_{KS}
Pentane	80.0±0.6	66.4±0.1	55.1±0.5
Hexane	80.5±0.7	66.4±0.1	55.1±0.5
Heptane	80.5±0.7	66.4±0.1	55.3±0.3
Octane	80.0±0.8	66.4±0.1	55.1±0.5
Nonane	80.7±0.6	66.5±0.4	54.8±0.2
2-Methylhexane		66.5±0.2	55.3±0.5
3-Methylhexane		66.5±0.2	55.1±0.5
2,3-Dimethylpentane		66.4±0.1	55.5±0.5
2,4-Dimethylpentane		66.4±0.1	55.0±0.4
2,2,3-Trimethylbutane		66.5±0.2	54.9±0.6
Benzene	81.2±0.4	66.4±0.5	54.8±0.2
Toluene	81.0±0.4	66.4±0.4	54.7±0.3
Ethylbenzene	81.2±0.8	66.5±0.5	55.1±0.5
p-Xylene	81.0±0.6	66.5±0.4	54.8±0.2
m-Xylene	80.2±0.6	66.5±0.4	55.1±0.5
o-Xylene	80.8±0.5	66.5±0.6	55.0±0.4
Cyclohexane	81.1±0.6	66.7±0.1	55.3±0.4
Average	80.7±0.4	66.5±0.1	55.1±0.2

[a] Uncertainties were estimated from the retention plots; the standard deviation is reported for the average value.

Table 2
Transition temperatures[a] (°C) for PDCBBS measured for different probes

	T_{SI}
Pentane	74.3±0.5
Hexane	73.2±0.6
Heptane	73.5±0.8
Octane	73.0±0.5
Nonane	72.8±0.6
2-Methylhexane	75.8±0.5
3-Methylhexane	75.5±1.0
2,3-Dimethylpentane	74.7±0.6
2,4-Dimethylpentane	75.2±0.4
2,2,3-Trimethylbutane	76.0±0.7
Benzene	73.8±0.8
Toluene	74.0±0.6
Ethylbenzene	74.0±0.7
p-Xylene	73.9±1.0
m-Xylene	75.2±0.7
o-Xylene	74.3±0.8
Cyclohexane	75.5±0.7
Average	74.4±1.0

[a] Uncertainties were estimated from the retention plots; the standard deviation is reported for the average value.

Table 3
Comparison of IGC transition temperatures with other methods

System	Transition	IGC	DSC	HSM[b]
HCB	K→N	59	58	58
	N→I	74	74	76
OCB	K→S_A	56	55	54.5
	S_A→N	67	66	67
	N→I	73	78	80
PDCBBS	S_A→I	73	73	74
MBHPT	K→S_C	57	53	57
	S_C→N*	110	113	112
	N*→ I	148–151[a]	147	147
PMMBTPS	S_C→I	70	67	63

Uncertainty is ±1–2 °C depending on the system.

N* is a chiral Nematic mesophase.

[a] Some probe dependence for this system.
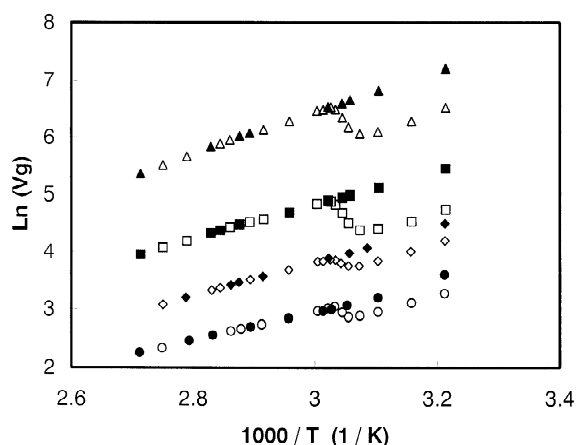
[b] From manufacturers' data.

Fig. 6. Retention diagram for HCB showing hysteresis (open points: heating cycle; closed points: cooling cycle) around the melting transition: ○,● pentane; □,■ hexane; △,▲ benzene; ◇,◆ ethyl benzene.

than hexane so that it dissolves into the solid at a slightly lower temperature [31]. Chow and Martire [35] compared IGC and DSC studies on two azoxy liquid crystals and reported no measurable adsorption effects from either interface above a film thickness of 100 nm. Witkiewicz [36] reported surface orientation effects up to a depth of 2 nm but in later work reported constant specific retention volumes above a stationary phase loading of above 5% [37]. Haky and Muschik [38] reported surface effects that lowered transition temperatures in a liquid crystal blend. However, the loading used was below the limits suggested above and well below that used in this work. Hence, we are confident that our IGC measurements represent the true transition temperatures.

On further consideration of the melting transition, there was considerable hysteresis. This is shown in Fig. 6 for HCB. Similar diagrams were obtained for OCB. The open points were obtained on heating and show a marked deviation at the melting point. However on cooling, indicated by the closed points, this is not seen and the compounds undergo supercooling. This has been observed several times in gas chromatography work [39] and the supercooled region has been reported to be sufficiently stable that it can be used to extend the separating power of these materials in analytical applications. This phase has always been regarded as a continuation of the mesophase to lower temperature [40]. However,

careful investigation showed that the supercooled phase exhibits properties which differ significantly from those of the equilibrium mesophase as will be described in the following section of this paper. Data for all probes exhibited different slopes about the supercooled and mesophase regions. The extent of the difference varied from probe to probe but the aromatics generally gave more marked changes. This indicates the supercooled phases in the LCs studied here are not simply extensions of the mesophases to lower temperature. After the compounds had been held at low temperatures for a period of a few days, the isothermal retention had again stabilised and values close to those measured in the crystalline phase were obtained.

The observation of this unstable supercooled region led us to consider the use of IGC to investigate the kinetics of crystallisation to the solid crystal phase. The timescale of the transition was ideal for us to determine whether the measurements were possible. The principle on which the measurements are based is related to that for measuring crystallinity in polymers. Here it is assumed that the probe samples amorphous regions of the polymer but cannot interact with crystalline regions. Thus, comparison of the retention time for a semi-crystalline material with that for a fully amorphous material (extrapolated from higher temperatures) allows esti-

mation of the degree of crystallinity. Recording the isothermal change in retention time as a function of time allows the kinetics to be followed. In work with LCs the principle relies on extrapolation of the retention of the mesophase to temperatures below the equilibrium melting (or in this case, freezing) temperature.

Crystallisation was studied at four temperatures below the metastable, supercooled region. The column was equilibrated in the middle of the mesophase temperature range and quickly quenched to the temperature of study. There was some variation in the temperature of the column during the crystallization of up to $\pm 0.5\,^{\circ}\text{C}$ in the worst case. Fig. 7 shows an example plot of the change in specific retention volume with time for three probes at $38.5\,^{\circ}\text{C}$. Two distinct regions can be seen. The first region occupies ~8–10 h during which time 30–35% of the liquid crystal has transformed into the solid state. This is followed by a longer period of time during which the remainder of the liquid crystal transformed to the solid state at a rate which slowed as complete crystallisation was approached.

Fig. 8 shows the mass fraction crystallinity, calculated [41] from Eq. (9), for the four temperatures, as measured by the heptane probe.

$$\text{Crystalline fraction} = \left(\frac{V_g^0(t=0) - V_g^0(t=\infty)}{V_g^0(t=t) - V_g^0(t=\infty)} \right) \quad (9)$$

where the retention volumes are recorded at the start of the crystallisation process and when equilibrium is reached (times $t=0$ and $t=\infty$, respectively) and any
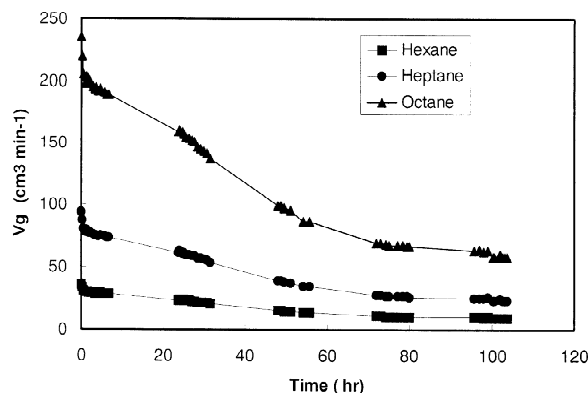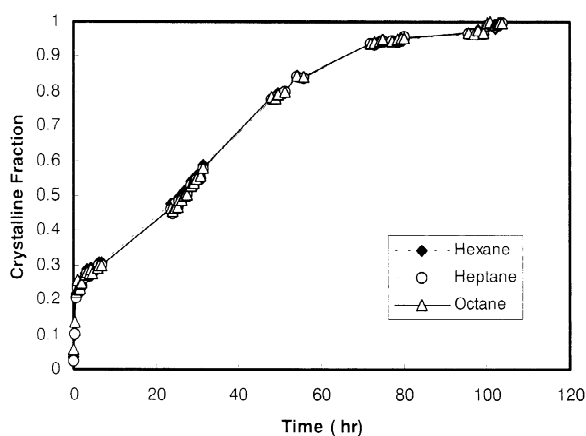

Fig. 8. Kinetics of crystallisation of the supercooled nematic phase of HCB.

time, t, during the process. Note that the calculation assumes the equilibrium state at long times was totally crystalline. The crystallisation process proceeded faster at higher temperature, as would be expected because of the greater thermal energy allowing faster rearrangement to the crystal form. The probe-to-probe reproducibility was good. The mass fraction crystallinity and its time variation can be used to investigate the mechanism of crystallisation and the method has been published previously [30].

This work has shown that IGC can be used to reliably measure the temperatures of a range of mesophase transitions in liquid crystals. It may be applied to a wide range of low-molar-mass or polymeric materials with a precision and accuracy comparable to other techniques. Although it is comparatively slow for transition temperature measurements alone, the technique has the potential to discern subtle phase changes that other techniques may not detect and also has the advantage of simultaneously measuring other data of interest, such as estimating the degree of crystallisation or measuring thermodynamic parameters of solution within a given phase, the latter being the subject of the following section of this paper.

4.2. Thermodynamics of interactions

In order to predict the properties of LC analytical stationary phases, it is of crucial importance to understand the nature and origin of their interactions

Fig. 7. Variation of retention volume with time during crystallisation of the supercooled nematic phase of HCB.
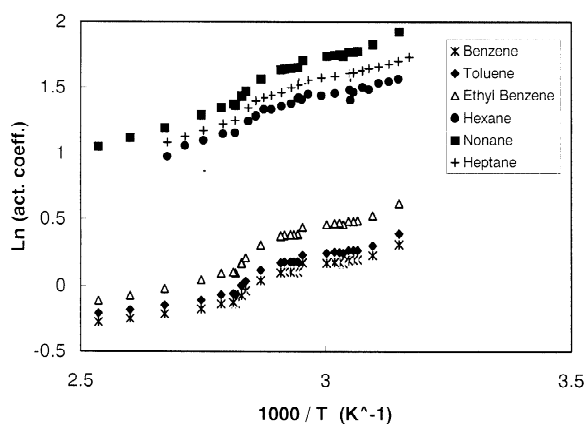
Fig. 9. Molar activity coefficients for OCB.

with the probes. To illustrate the work, consider the results for OCB which displays a smectic A phase, the same as displayed by PDCBBS.

A selection of the molar activity coefficients is shown in Fig. 9. The data, primarily the slopes of the graphs in each mesophase region, were also used to calculate enthalpies and entropies of solution according to Eq. (2) for the probes and these are shown in Table 4. Some trends from the data are readily apparent. For example, the activity coefficients are generally lower in the isotropic (high temperature)

phase than in the ordered mesophases (when extrapolated to the same temperatures to account for the effect of temperature). This shows that the ordering within the mesophase has an unfavourable effect on the mixing. The values of γ for the aromatic probes are lower than the aliphatics indicating that the former are much more compatible. This also suggests that the cyanobiphenyl moiety is more important in terms of its interactions than the alkyl chain part of the LC.

The enthalpies of solution reveal that the largest values are given for the S_A mesophase; the same holds for the entropies of solution. Low values of activity coefficient are a result of strong interactions and/or little restriction of the probe molecule in solution. The partial molar entropy change of solution describes the loss of entropy the probe suffers on transferring from the gas phase to the infinitely dilute solution. Large, negative values indicate a large restriction on probe movement in the infinitely dilute solution but strong interactions between probe and liquid crystal will also lower this entropy. This forms the most ordered mesophase and it is reasonable to expect the largest interactions to take place. The same argument explains the fact that the lowest values are generally given by the disordered isotropic phase. There are differences between the S_A and the

Table 4
Partial molar solution values for OCB

Probe	Isotropic (90 °C)		Nematic (73 °C)		Smectic A (60 °C)		$S_A^{supercool}$ (48 °C)	
	$-\Delta H^{sol}$	$-\Delta S^{sol}$	$-\Delta H^{sol}$	$-\Delta S^{sol}$	$-\Delta H^{sol}$	$-\Delta S^{sol}$	$-\Delta H^{sol}$	$-\Delta S^{sol}$
Pentane	14.9 (1.8)	61.5 (1.5)	15.0 (3.2)	62.0 (2.4)	21.5 (3.4)	81.5 (0.2)	18.3 (1.3)	71.5 (1.5)
Hexane	20.0 (0.9)	68.8 (0.7)	17.7 (1.8)	63.1 (0.1)	24.4 (1.7)	82.7 (1.4)	22.0 (2.0)	75.3 (1.2)
Heptane	23.0 (0.2)	70.7 (0.1)	20.7 (1.4)	64.9 (0.0)	26.9 (1.1)	83.1 (0.8)	26.9 (0.5)	82.8 (0.4)
Octane	24.9 (0.2)	69.6 (0.1)	23.9 (1.2)	67.3 (0.0)	31.2 (0.9)	88.8 (0.7)	27.1 (2.9)	75.9 (0.2)
Nonane	31.2 (0.2)	79.9 (0.2)	28.2 (1.8)	72.0 (1.7)	39.4 (1.0)	105.1 (0.7)	30.8 (0.7)	78.5 (0.5)
2-Methylhexane	21.0 (1.0)	65.8 (0.4)	17.3 (1.6)	56.0 (1.2)	18.6 (3.2)	59.4 (2.5)	24.7 (0.4)	77.3 (0.4)
3-Methylhexane	20.7 (0.5)	64.3 (0.7)	17.2 (0.7)	54.9 (0.5)	16.4 (3.5)	52.1 (2.0)	25.9 (1.4)	80.5 (1.1)
2,3-Dimethylpentane	19.6 (0.2)	61.4 (0.1)	16.8 (1.7)	54.0 (0.9)	17.4 (3.6)	55.4 (2.7)	24.6 (0.5)	76.9 (0.5)
2,4-Dimethylpentane	18.8 (1.4)	62.2 (1.2)	17.3 (2.5)	58.7 (1.3)	17.7 (3.2)	59.5 (2.6)	23.9 (0.7)	77.9 (0.7)
2,2,3-Trimethylbutane	20.3 (0.8)	65.4 (0.9)	15.2 (0.8)	51.7 (0.6)	15.8 (3.7)	53.3 (3.1)	22.4 (0.6)	72.6 (0.6)
Cyclohexane	19.4 (1.1)	60.6 (1.2)	15.6 (1.9)	50.5 (0.1)	21.8 (1.3)	68.6 (1.1)	23.2 (0.0)	72.8 (0.0)
Benzene	25.6 (0.2)	71.4 (0.4)	18.2 (1.8)	51.2 (1.4)	31.4 (0.9)	90.2 (0.6)	21.9 (1.0)	61.1 (0.7)
Toluene	29.7 (0.2)	75.6 (0.5)	22.2 (2.0)	55.2 (0.2)	33.8 (0.7)	89.4 (0.6)	25.7 (1.0)	64.5 (0.7)
Ethylbenzene	31.3 (0.2)	74.6 (0.6)	24.1 (2.2)	55.1 (0.2)	36.9 (0.8)	92.8 (0.6)	28.6 (1.0)	67.4 (0.7)
o-Xylene	33.6 (0.2)	77.8 (0.7)	25.9 (2.2)	56.8 (0.2)	38.6 (0.8)	94.0 (0.6)	30.3 (0.9)	68.6 (0.7)
m-Xylene	34.2 (0.9)	81.1 (1.7)	28.9 (0.2)	67.3 (0.1)	35.7 (1.2)	87.6 (0.6)	30.1 (1.8)	70.3 (0.5)
p-Xylene	33.8 (0.2)	80.2 (0.6)	26.6 (2.0)	60.4 (0.2)	38.7 (0.9)	96.0 (0.6)	29.9 (0.9)	69.3 (0.7)

Enthalpies in kJ mol^{-1} and entropies in J mol^{-1} K^{-1}. Uncertainties in parentheses.

supercooled S_A regions confirming the comments above that the latter may not simply be a lower temperature extrapolation of the former phase. The rising values among the alkane probes are a result of increasing interaction in the bigger molecules (due to the increasing polarisability) and the increased difficulty of accommodating larger molecules within the LC ordering, particularly in the layered structures. Comparing the thermodynamic parameters of the heptane isomers between different phases and mesophases of HCB reveals very similar trends to those observed for the *n*-alkanes above but there is little difference in the entropies of solution. This indicates that the behaviour is largely governed by interaction between probe and liquid crystal molecules rather than restriction of the probe molecule by the stationary phase. The isomers present a variety of molecular shapes from the globular 2,2,3-trimethylbutane to the flexible heptane chain. An alternative, more speculative explanation would be that these compounds do not enter and hence disrupt the ordered mesophases. However, this would need more investigation.

The activity coefficients, on a weight fraction basis, were calculated for PDCBBS and again showed the trend that the values, as well as those for ΔH^{sol} and ΔS^{sol}, were larger in the smectic A phase

than the isotropic. Hence, it is likely that the trends in the thermodynamic parameters for PDCBBS were governed by the interaction strengths between probes and mesogen. The ΔH^{sol} were of a similar magnitude to OCB and generally considerably higher than those reported for poly(dimethyl siloxane) (PDMS), again indicating that the mesogen was governing the solution behaviour.

In order to further assist comparison between the polymeric and low-molar-mass versions of the mesogens, Flory–Huggins interaction parameters were calculated and are shown for both the smectic A and isotropic phases in Table 5. The values for PDCBBS are in all cases closer to those for the LC equivalent than the PDMS backbone. This implies the PDCBBS-probe solution is governed by the mesogen rather than the backbone both in the mesophase and the isotropic phase although the effect is greater in the former. This is further illustrated by the temperature dependence of χ shown for benzene and hexane as probes in Fig. 10. It is clear that the values are dominated by the mesogen rather than the polymer backbone. Although only illustrated for two probes, this was a general phenomenon; retention in the LCP mirrored that in the equivalent LCs rather than the polymer. This knowledge is especially useful since it allows us

Table 5

Comparison of interaction parameters for PDCBBS and OCB in the smectic and isotropic phases with PDMS

	Smectic A (70 °C)			Isotropic (85 °C)		
	PDCBBS	PDMS	OCB	PDCBBS	PDMS	OCB
Pentane	1.22	0.34	1.53	0.97	0.32	1.40
Hexane	1.25	0.37	1.60	0.96	0.35	1.39
Heptane	1.29	0.40	1.65	0.98	0.38	1.41
Octane	1.31	0.45	1.70	0.95	0.44	1.43
Nonane	1.29	0.51	1.71	0.97	0.50	1.45
2-Methylhexane	1.27	0.37	1.48	0.98	0.36	1.22
3-Methylhexane	1.27	0.37	1.46	0.95	0.35	1.19
2,3-Dimethylpentane	1.21	0.33	1.42	0.92	0.31	1.16
2,4-Dimethylpentane	1.30	0.34	1.49	1.02	0.32	1.26
2,2,3-Trimethylbutane	1.19	0.29	1.41	0.92	0.27	1.16
Cyclohexane	1.10	0.40	1.30	0.82	0.36	1.03
Benzene	0.57	0.54	0.59	0.27	0.44	0.31
Toluene	0.54	0.56	0.55	0.28	0.52	0.31
Ethylbenzene	0.62	0.59	0.66	0.31	0.55	0.39
p-Xylene	0.43	0.66	0.50	0.22	0.62	0.27
m-Xylene	0.57	0.70	0.57	0.24	0.66	0.30
o-Xylene	0.52	0.73	0.53	0.21	0.70	0.27

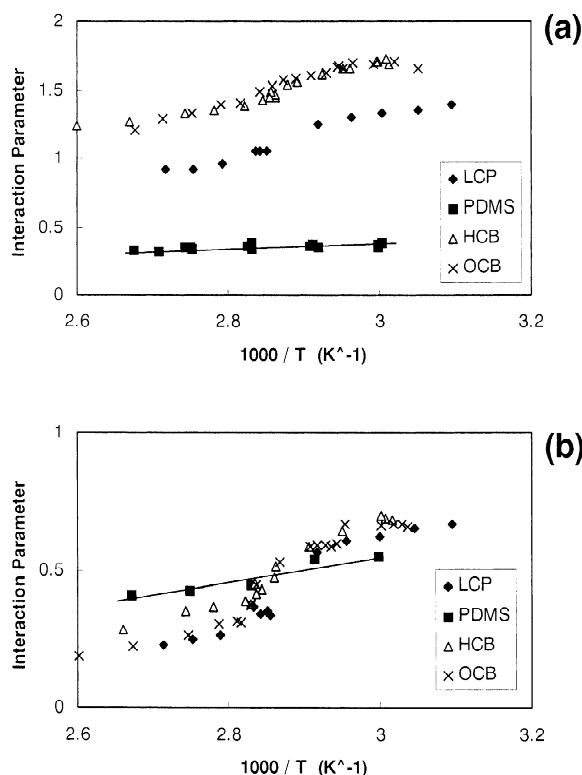*G.J. Price et al. / J. Chromatogr. A 969 (2002) 193–205*

203

(a)

(b)

Fig. 10. Comparison of interaction parameters for (a) hexane and (b) benzene in HCB, OCB, PDCBBS and PDMS.

essentially to separate the behaviour of the two components of the stationary phase. Separation (governed primarily by the interaction thermodynamics) can be gained by suitable mesogenic groups while other properties such as diffusivity, glass transition can be varied by the polymer backbone.

The purpose of this paper is not to give a complete thermodynamic interpretation of the data [42] but the foregoing discussion will illustrate the information that can be obtained. In considering a specific analytical separation, the balance between interaction energies and molecular shape, etc., can be used to engineer a particular phase.

4.3. Mixtures of LCs and polymers

In chemical terms, the LCP could be thought of as being equivalent to a mixture of the low-molar-mass LC with the siloxane polymer. Thus, it was of interest to compare the chromatographic behaviour
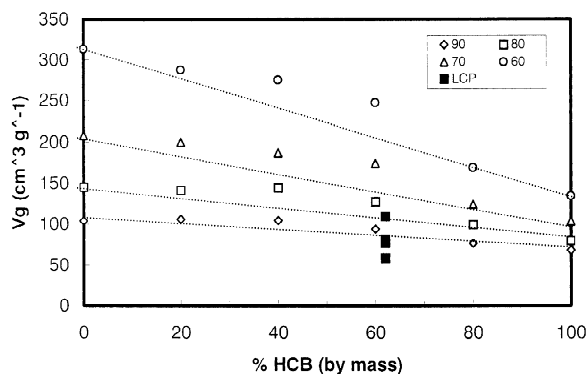

Fig. 11. Comparison of retention in mixtures of PDMS and HCB at the indicated temperatures (°C) with that in PDCBBS.

of the two systems. In general, single component stationary phase systems are preferred but there has been considerable interest in mixed component systems [43]. The retention volumes for four probes in several mixtures of HCB and PDMS are shown in Fig. 11.

It was shown some years ago that a linear variation with composition would arise if the components were immiscible. In this case, it is clear that the components do mix although the interactions are unfavourable. Positive interaction parameters between the components were calculated [44]. It is interesting to compare the V_g^0 values for PDCBBS compared with the binary stationary phase results. Consideration of the structure of PDCBBS (confirmed by NMR spectroscopy) leads to an effective composition of 62% (w/w) mesogen. These values are also shown in Fig. 11. Clearly the values for PDCBBS are considerably lower than those for the binary stationary phase. This reflects the structure of PDCBBS where the mesogen and polysiloxane backbone are compelled to interact more intimately than the individual components, HCB and PDMS, because the mesogen is now chemically bonded to the polysiloxane backbone. From an analytical chromatography viewpoint, this is advantageous since the lower retention will lead to higher efficiencies on the column.

5. Conclusions

This paper has illustrated some of the fundamental

measurements that have been made on a range of LC systems with the aim of fully characterising their behaviour. We have shown that we can monitor changes in retention due to small and subtle changes in molecular order and determine the phase transition temperatures with accuracy comparable with more established methods. We have been able to study the supercooled mesophase but our work suggests that this may not be a simple lower temperature extension of the mesophase and displays different chromatographic properties. The kinetics of phase transitions can be monitored and the nature and origin of probe-stationary phase interactions can be measured and understood. Finally, consideration of the properties of polymeric stationary phases can be correlated in terms of the behaviour of the related low-molar-mass mesogens. This work forms the basis of the design and rationalisation of LC stationary phases for analytical purposes and related publications will deal with the separation properties of these and related LC compounds.

6. Nomenclature

γ^∞	molar activity coefficient at infinite dilution
ΔG^{sol}	Gibbs energy of solution
ΔH^{sol}	molar enthalpy of solution
ΔS^{sol}	molar entropy of solution
χ_0	Flory–Huggins interaction parameter
p^0	saturated vapour pressure of probe
Ω^∞	weight fraction activity coefficient at infinite dilution
B_{11}	second virial coefficient of the probe vapour
F'	carrier gas flow-rate at STP
J	flow-rate correction factor
M_1	molar mass of the probe
M_2	molar mass of the stationary phase
T	column temperature
V_{g}^0	specific retention volume
V_1^0	molar volume of the probe
W	mass of stationary phase on the column.
DSC	differential scanning calorimetry
HCB	4-n-hexyloxy($4'$-cyanobiphenyl)

HSM	hot stage microscopy
I	isotropic liquid phase
MBHPT	(2-methylbutyl)(4-hexyloxy-phenyl)terephthalate
N	liquid crystalline nematic phase
OCB	4-n-octyloxy($4'$-cyanobiphenyl)
PDCBBS	poly(dimethyl–co-methyl(4-cyanobiphenyloxy)butylsiloxane)
PDMS	poly(dimethyl siloxane)
PMMBTPS	poly(methyl(2-methylbutyl-terephthaloylphenoxypentyl)-siloxane)
S_A	liquid crystalline smectic A phase
S_C	liquid crystalline smectic C phase

References

[1] C.B. McArdle (Ed.), Side Chain Liquid Crystal Polymers, Blackie, London, 1989.

[2] P.J. Collings, Liquid Crystals: Nature's Delicate Phase of Matter, Hilger, Bristol, 1990.

[3] J.E.G. Lipson, J.E. Guillet, in: J.V. Dawkins (Ed.), Developments in Polymer Characterisation 3, Applied Science, Barking, 1982, Chapter 2.

[4] Z.Y. Al-Saigh, J.E. Guillet, in: R. Meyers (Ed.), Encyclopedia of Analytical Chemistry: Instrumentation and Applications, Wiley, Chichester, 2000, p. 7759.

[5] J.R. Conder, C.L. Young, Physicochemical Measurement by Gas Chromatography, Wiley, Chichester, 1979.

[6] D.H. Everett, Trans. Farad. Soc. 61 (1965) 1637.

[7] D. Patterson, Y.B. Tewari, H.P. Schreiber, J.E. Guillet, Macromolecules 4 (1971) 356.

[8] J.E. Haky, G.M. Muschik, J. Chromatogr. 214 (1981) 161.

[9] H. Kelker, Ber. Bunsenges Phys. Chem. 67 (1963) 698.

[10] G.M. Janini, G.M. Muschik, C.M. Hanlon, Mol. Cryst. Liq. Cryst. 53 (1979) 15.

[11] Z. Witkiewicz, M. Pietrzyk, R. Dabrowski, J. Chromatogr. 177 (1979) 189.

[12] Z. Witkiewicz, J. Chromatogr. 251 (1982) 311.

[13] Z. Witkiewicz, J. Chromatogr. 466 (1989) 37.

[14] Z. Witkiewicz, J. Mazur, LC·GC 8 (3) (1989) 224.

[15] R.J. Laub, Side Chain Liquid Crystal Polymers, Blackie, London, 1989, Chapter 14.

[16] G.M. Janini, G.M. Muschik, H.J. Issaq, R.J. Laub, Anal. Chem. 60 (1988) 1119.

[17] L.C. Chow, D.E. Martire, J. Phys. Chem. 75 (1971) 2005.

[18] D.E. Martire, C. Yan, J. Phys. Chem. 96 (1992) 7510.

[19] D.E. Martire, J. Chromatogr. 406 (1987) 27.

[20] Y. Chao, D.E. Martire, Anal. Chem. 64 (1992) 1246.

[21] S. Ghodbane, G.A. Oweimreen, G.C. Lin, D.E. Martire, J. Phys. Chem. 83 (1979) 2111.

[22] S. Ghodbane, G.A. Oweimreen, D.E. Martire, J. Chromatogr. 556 (1991) 317.

G.J. Price et al. / J. Chromatogr. A 969 (2002) 193–205

205

[23] G.J. Price, I.M. Shillcock, Polymer 34 (1993) 85.
[24] F. Gritti, G. Felix, M.F. Achard, F. Hardouin, J. Chromatogr. A 893 (2000) 359.
[25] M. Romansky, J.E. Guillet, Polymer 35 (1994) 584.
[26] M. Romansky, P.F. Smith, J.E. Guillet, A.C. Griffin, Macromolecules 27 (1994) 6297.
[27] G. Tovar, P.J. Carreau, H.P. Schreiber, Colloids Surfaces A–Physicochem. Eng. Aspects 161 (2000) 213.
[28] Selected Values of the Properties of Hydrocarbons and Related Compounds, TRC, College Station, TX, 1965, data project, see also subsequent revisions.
[29] A.T. James, A.J.P. Martin, Biochem. J. 50 (1952) 679.
[30] G.J. Price, I.M. Shillcock, Can. J. Chem. 73 (11) (1995) 1883.
[31] M.A. Llorente, C. Menduina, A. Horta, J. Polym. Sci. Polym. Phys. Ed. 17 (1979) 189.
[32] Z. Witkiewicz, J. Chromatogr. 251 (1982) 311.

[33] W. Marciniak, Z. Witkiewicz, J. Chromatogr. 207 (1981) 333.
[34] M. Romansky, J.E. Guillet, Abstr. Pap. Am. Chem. Soc. 204 (1992) 231.
[35] L.C. Chow, D.E. Martire, J. Phys. Chem. 73 (1969) 1127.
[36] Z. Witkiewicz, J. Chromatogr. 188 (1980) 107.
[37] W. Marciniak, Z. Witkiewicz, J. Chromatogr. 207 (1981) 333.
[38] J.E. Haky, G.M. Muschik, J. Chromatogr. 238 (1982) 367.
[39] H. Kelker, Z. Anal. Chem. 198 (1963) 254.
[40] S. Wasik, S. Chester, J. Chromatogr. 122 (1976) 451.
[41] D.G. Gray, J.E. Guillet, Macromolecules 4 (1971) 129.
[42] G.J. Price, I.M. Shillcock, Phys. Chem. Chem. Phys., submitted.
[43] G.J. Price, Adv. Chromatogr. 28 (1989) 113.
[44] D.D. Deshpande, D. Patterson, H.P. Schreiber, C.S. Su, Macromolecules 7 (1974) 530.